Tumor Cure Probability During α-RIT of Ovarian Cancer with Different Radiation Sensitivity

J. ELGQVIST[1], B.R. JOHANSSON[2], K. PARTHEEN[3] and A. DANIELSSON[1]

[1]*Institute of Clinical Sciences,* [2]*Electron Microscopy Unit, Institute of Biomedicine and* [3]*Department of Obstetrics and Gynecology, Sahlgrenska Academy, University of Gothenburg, Gothenburg, Sweden*

Abstract. *Purpose: To calculate the tumor cure probability (TCP) and metastatic cure probability (MCP) during α-radioimmunotherapy (α-RIT) of small ovarian cancer tumors with cells of different radiation sensitivity. Materials and Methods: An in-house-developed biokinetic model and a Monte-Carlo program were used to calculate the cumulative activity on tumor cell surfaces and the specific energy to tumor cell nuclei, respectively. An in-house-developed computational model was used to calculate the TCP and MCP as a function of assumed radiation sensitivities, expressed as D_{37}, of the tumor cells. The calculations were performed using various assumptions regarding the activity distribution in measured tumors and used the α-particle energies emitted from astatine-211 (^{211}At). Regarding the calculations of the cumulative activity on each cell surface, the number of antigenic sites expressed by NIH:OVCAR-3 cells for the mAb MX35 F(ab')2 was used. To illustrate the tumor growth at the peritoneum in nude mice, scanning electron microscopy images were used. Results: In the case of a maximum diffusion depth of 30 μm for the activity in the tumors, the TCP was high for D_{37} values not exceeding ~4.3, ~2.9, ~1.8, and ~0.8 Gy for 200, 100, 50, and 25 kBq ^{211}At-MX35 F(ab')2 four weeks after cell inoculation, respectively. In order to achieve complete remission of the metastatic disease in mice (i.e. MCP=1), the D_{37} value should not exceed ~2.2, ~1.3, ~0.6, and ~0.3 Gy when injecting 200, 100, 50, or 25 kBq, respectively, assuming a maximum diffusion depth of 30 μm for the activity in the tumors. Conclusion: The radiation sensitivity, expressed as D_{37}, of tumor cells subjected to α-RIT could be decisive for therapeutic outcome, expressed as TCP or MCP, when treating small tumors of ovarian cancer.*

Correspondence to: Jörgen Elgqvist, Ph.D., Department of Oncology, Sahlgrenska Academy, University of Gothenburg, Sweden. e-mail: jorgen.elgqvist@gu.se

Key Words: Tumor cure probability, radiation sensitivity, ovarian cancer, radioimmunotherapy, astatine.

Ovarian cancer is frequently lethal because of residual disease metastasized to the peritoneal surfaces, notwithstanding complete clinical remission after surgery and systemic chemotherapy. Conventional platinum-based chemotherapy is often ineffective as a result of cellular resistance mechanisms. External whole-abdominal irradiation has only shown limited success because of the toxic effects on the intestines. However, monoclonal antibodies (mAbs) have made targeted radiation therapy possible, offering the chance to increase the absorbed dose to the tumor, while remaining below the toxicity level of surrounding normal tissues. Several genes are known to be involved in the development of ovarian cancer. In hereditary cases, the most common mutated genes are the tumor suppressor genes *BRCA1* and *BRCA2*, and the DNA repair genes *MSH2* and *MLH1* (1-2). The most frequently studied tumor suppressor genes in sporadic cases of ovarian cancer encode the proteins p53 and CDKN2A (3-4). Tumor suppressor p53 is a transcription factor that plays an essential role in the cell cycle regulation. It is however often mutated to a defective form, which may be highly expressed in cancer cells, and contributes to cell transformation and malignancy. Mutations and deletions in such tumor suppressor genes may cause loss of protective functions in the regulation of the cell through the events of replication and division and results in altered response to radiation damage, resulting in either radiosensitive or radioresistant phenotypes. The radiosensitivity of tumor cells varies and is a critical determinant of the probability of cure in patients receiving radiotherapy for cancer (5). For example, the relationship between different types of *p53* mutations and the degree of radiation sensitivity *in vitro* was recently published (6). The authors showed that the sensitivity of Saos-2 cells to ionizing radiation varied greatly with the type of mutation. Findings like these make it of outmost importance to investigate how the therapeutic outcome after targeted radiotherapy will be affected by the difference in radiosensitivity of ovarian cancer cells.

Studies performed to investigate the therapeutic efficacy of β-particle emitters, mostly yttrium-90 (^{90}Y) and iodine-131 (^{131}I) labeled mAbs, in animals and humans with ovarian cancer have shown limited success (7-17). Some studies with α-particle emitters have also been carried out

(18, 19). In the present study, the tumor cure probability (TCP) and metastatic cure probability (MCP) of the α-particle emitter ^{211}At, with a half-life of 7.21 h, mean range in tissue of ~62 μm, and a mean linear energy transfer (LET) of ~111 keV/μm, were calculated. The role of the radiation sensitivity of the tumor cells, expressed as D_{37}, on the therapeutic outcome was also calculated. We have previously investigated therapeutic efficacy using both intact IgG1 mAbs MOv18 and MX35, as well as fragmented mAbs (MX35 F(ab')$_2$ and nonspecific Rituximab F(ab')$_2$) in the treatment of microscopic disease of ovarian cancer in nude mice (20-24). In a previous study (25), we investigated the TCP for a fixed value of the radiation sensitivity of the tumor cells.

In a metastatic disease such as ovarian cancer, the tumors may vary in size, and to obtain complete remission all tumors must be eradicated. In the present study, we have further developed an *in vivo* TCP model based on measured tumor sizes (24). Based on a previous estimation of the tumor size distribution (25), the MCP was also calculated and plotted as a function of the radiation sensitivity, expressed as D_{37}, of the tumor cells in mice, D_{37} being the absorbed dose required for a growth inhibition corresponding to 0.37.

Materials and Methods

Radiation dosimetry. Specific energy values of radiation to the nuclei of tumor cells, regarding various assumptions of the tumor size and activity distribution, were used from published data (25). A previously described computer program (26) was used for the dosimetry of the tumors. The program uses stopping power values of α-particles in liquid water (27) for Monte-Carlo-derived dosimetry and was designed to calculate the energy deposition in a defined target volume, a 7.2-μm radius sphere, simulating a single tumor cell nucleus embedded at various depths in the tumor. For each tumor size, five target positions were selected along the central axis of the tumor. Tumor sizes at the time of treatment four weeks after cell inoculation were estimated by analyzing scanning electron microscopy (SEM) images. The cell packing ratio was assumed to be 1.0 in each tumor, *i.e.*, assuming no intercellular space. The calculations were performed for spherical tumors with radii, r_{tumor}, equal to 30, 45, and 95 μm. Four activity distributions were assumed: (i) activity homogeneously distributed at the antigenic sites throughout the whole tumor, (ii) activity homogeneously distributed at the antigenic sites within a maximum diffusion depth of 30 μm, (iii) activity distributed only at the antigenic sites at those cell surfaces defining the surface of the tumor, and (iv) activity freely circulating around the tumor without specific binding to antigenic sites. For the calculation of the number of antigenic sites exposed on the tumor surface, a 'cobblestone' surface was assumed, giving twice the tumor surface area compared with calculations for a smooth surface. The cumulative activity on a tumor cell was calculated with an in-house developed compartmental model (23). Regarding the mAb distribution described above in which limited penetration of the activity into the tumors was assumed, a diffusion model was adopted. This model was incorporated because a previous study had indicated that a homogeneous distribution of the activity in the tumors was inconsistent with the therapeutic results (24). The diffusion model was based on the assumption of a binding site barrier (28). A maximum diffusion depth (d_{diff}) of 30 μm in the tumors was assumed in those cases. The activity was assumed to diffuse freely to d_{diff} momentarily after the injection into the abdominal cavity.

Tumor cure probability model. Based on measured tumor sizes four weeks after intraperitoneal inoculation of ~1×10^7 NIH:OVCAR-3 cells in mice, cores and shells were defined for three tumor sizes, with a radius equal to 30, 45, or 95 μm (25). The 95-μm tumor corresponds to the largest tumors found at the time of the intraperitoneal treatment four weeks after the cell inoculation. The reason for defining cores and shells was that we expected an inhomogeneous absorbed dose distribution in the tumors, and this definition enabled us to calculate the probability for cell survival for different tumor sizes, activity distributions, and amounts of injected activity.

For the 30-μm tumor, the core was defined as a sphere with a radius of 12 μm. Two shells were defined for this tumor size, one ranging from 12 to 21 μm from the center, and one ranging from 21 to 30 μm from the center. For the 45-μm tumor, the core was defined as a sphere with a radius of 9 μm. Four shells were defined 9-18, 18-27, 27-36, and 36-45 μm from the center. For the 95-μm tumor, the core was defined as a sphere with a radius of 23 μm. Eight shells were defined 23-32, 32-41, 41-50, 50-59, 59-68, 68-77, 77-86, and 86-95 μm from the center.

Polynomial fits were made to the specific energy calculations, representing the three tumor sizes (30, 45, and 95 μm), the four activity levels (200, 100, 500, and 25 kBq), and the four irradiation geometries (see above). The mean absorbed dose was assigned to the corresponding tumor core and shell.

The number of surviving cells in each tumor (n_s), consisting of m compartments (*i.e.* the core + the shells), was calculated as:

$$n_s = n_{cell} \cdot \sum_{i=1}^{m} VF_i \cdot S_i = n_{cell} \cdot \sum_{i=1}^{m} VF_i \cdot e^{-\alpha D_i}$$

(Eqtn. 1)

where n_{cell} is the total number of cells in the tumor, VF_i is the volume fraction of the i^{th} core or shell, S_i is the surviving fraction of cells in this i^{th} core/shell receiving the mean absorbed dose D_i, and α is the parameter describing the cells' radiation sensitivity ($1/D_{37}$ [Gy^{-1}]). D_{37} being the absorbed dose required for a growth inhibition corresponding to 0.37.

Because a packing ratio of 1.0 was assumed, the VF_i represents the fraction of n_{cell}, for each tumor size, belonging to each core and shell.

The TCP for each tumor, consisting of m compartments (*i.e.*, the core plus the shells) and n_i cells in each core or shell, was calculated for the different activity levels and irradiation geometries from:

$$TCP = \prod_{i=1}^{m} (1 - S_i)^{n_i}$$

(Eqtn. 2)

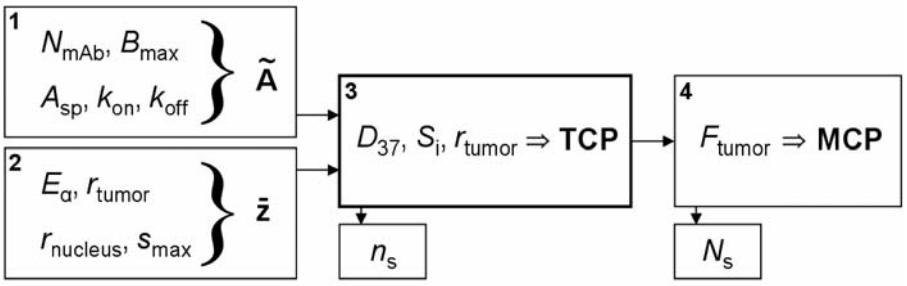

Figure 1. *Computational model enabling the calculation of TCP and MCP. Compartment 1 calculates the cumulative activity at a tumor cell surface using the parameters N_{mAb}=the number of antibodies injected in the abdominal cavity, B_{max}=the number of antigenic sites on one tumor cell, A_{sp}=the specific activity of the injected radioimmunocomplex, k_{on}=the rate at which the antibodies bind to the antigenic sites, and k_{off}=the rate at which the antibodies will be released from the antigenic sites. Compartment 2 calculates the mean specific energy delivered to tumor cell nuclei situated at various depths in the tumor using the parameters E_α=the energies of the emitted α-particles from ^{211}At, r_{tumor}=the radius of the relevant tumor, $r_{nucleus}$=the radius of the tumor cell nucleus, s_{max}=the maximum path length of the emitted α-particles from ^{211}At. Compartment 3 calculates the TCP using the parameters D_{37}=absorbed dose resulting in 37% of the tumor cells surviving, S_i=surviving fraction, r_{tumor}=the radius of the relevant tumor. Compartment 4 calculates the MCP using F_{tumor}=the estimated distribution function of the number of tumors of different sizes present in an animal. Compartment 3 and 4 also enables the computation of n_s (the number of surviving cells in a particular tumor) and N_s (the total number of surviving cells in an animal), respectively.*

where S_i is the surviving fraction of cells in the i^{th} core/shell receiving the mean absorbed dose D_i.

The total number of 30-, 45-, and 95-μm tumors present in each tissue specimen was estimated by analyzing the SEM images and used to calculate the MCP (Equation 3) for an animal, for each activity level and irradiation geometry, for a disease containing k different tumors with m_h number of 30-, 45-, and 95-μm tumors, respectively:

$$MCP = \prod_{h=1}^{k} (TCP_h)^{m_h} \qquad \text{(Eqtn. 3)}$$

where TCP_h is the tumor cure probability for the h^{th} tumor size.

Figure 1 shows a schematic diagram of the computational model used to calculate the TCP and MCP, including its most important parameters.

Scanning electron microscopy of tumors in mice. Specimens for ultrastructural analysis were obtained from mice anesthetized with Metofane (Mallinckrodt Veterinay Inc., Mundelein, IL, USA) four weeks after cell inoculation. The thoracic cavity was exposed and the heart root was clamped to arrest blood flow, after which an intraperitoneal injection (5 ml) of a mixture of 2.5% glutaraldehyde, 2% paraformaldehyde, and 0.01% sodium azide in 0.05 mol/l sodium cacodylate (pH 7.2) was given. After 10 min of primary fixation, the abdominal cavity was exposed and specimens, including peritoneal lining and jejunum (including mesenteries), were harvested by dissection. Specimens were further fixed overnight in the aldehyde mixture. After rinsing in 0.15 M cacodylate, specimens for electron microscopy were subjected to the osmium-thiocarbohydrazide-osmium (OTOTO) postfixation technique (29). Dehydration followed in a series of ethanol, finally replaced by two changes of hexamethyldisalazane, which was allowed to evaporate under a fume hood. The dried specimens were mounted on aluminum stubs and were examined in a Zeiss 982 Gemini field-emission scanning electron microscope after coating with palladium in an Emitech 550 sputter coater. Digital images were collected at a resolution of 1024×1024 pixels. Each tissue specimen (~16 mm^2) was examined in the electron microscope.

Results

Tumor cure probability (TCP). In Figure 2, the TCP as a function of D_{37} for each tumor size, irradiation geometry, and activity level is plotted. It can be seen that for the smallest tumor investigated (r_{tumor}=30 μm) the TCP was generally high for all values of D_{37}, activity levels, and irradiation geometries, except for the case of unbound activity. In that case, the limit of the D_{37} for achieving TCP=1 (and hence n_s=0) was ~1.8, ~1.3, ~0.3, and ~0 Gy for 200, 100, 50, and 25 kBq ^{211}At-MX35 F(ab')$_2$, respectively. The corresponding D_{37} values for the 45-μm tumor were ~0.9, ~0.3, ~0.1, and ~0 Gy. Regarding the largest tumors found four weeks after cell inoculation (r_{tumor}=95 μm) the situation was worse. Due to the relatively short path length of the emitted α-particles in tissue (~71 μm), the irradiation geometries in which the activity, was only situated on the surface of the tumor or completely unbound circulating around the tumor, the TCP would be equal to zero for all D_{37} values. In the case of limited diffusion of the activity the TCP was high (*i.e.* $n_s \approx 0$) for D_{37} values not exceeding ~4.3, ~2.9, ~1.8, and ~0.8 Gy for 200, 100, 50, and 25 kBq ^{211}At-MX35 F(ab')$_2$, respectively. In the case of a homogeneous activity distribution in the tumors the TCP started to decline apparently only at the 25 kBq level and for D_{37} values exceeding ~4 Gy.

Metastatic cure probability (MCP). In Figure 3, the MCP as a function of D_{37} for each irradiation geometry and activity level is plotted. The curves for the cases in which the activity

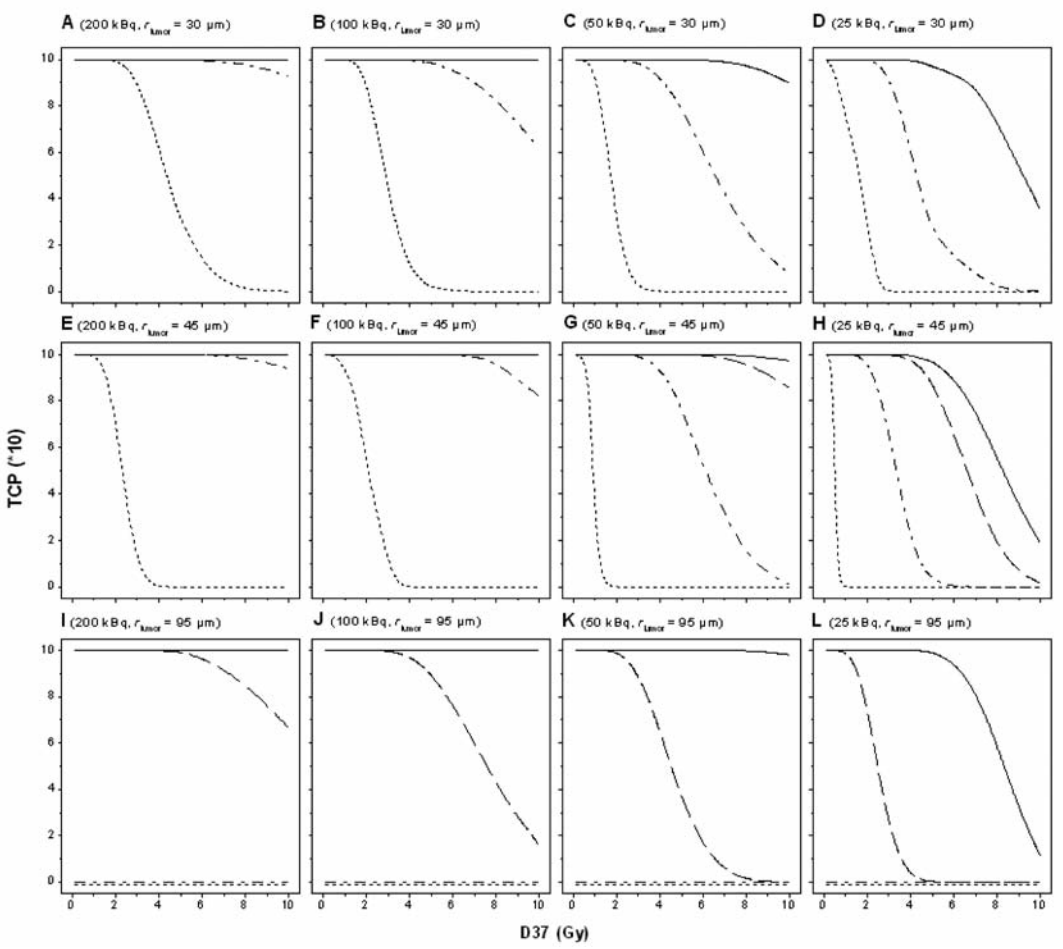

Figure 2. *Tumor cure probability (TCP) as a function of D_{37} for each studied tumor size, depending on irradiation geometry and activity level. Solid line (—): activity homogeneously distributed at all antigenic sites throughout the whole tumor. Dashed line (– –): activity distributed only at antigenic sites located within the assumed maximum diffusion depth (30 µm). Dash-dotted line (– · –): activity distributed only at antigenic sites on the surface of the tumor. Dotted line (· · ·): activity unbound and freely circulating around the tumor. Rows represent tumors with a defined size, i.e. A-D: tumor radius equal to 30 µm, E-H: tumor radius equal to 45 µm, I-L: tumor radius equal to 95 µm. Columns represent the same level of injected activity of ^{211}At-MX35 F(ab')2, i.e. A, E, I: 200 kBq; B, F, J: 100 kBq; C, G, K: 50 kBq; and D, H, L: 25 kBq.*

was distributed only at antigenic sites on the surface of the tumor or unbound and freely circulating around the tumor were omitted due to the fact that the MCP is zero for all values of D_{37} in those cases. This is explained by the limited path length of the α-particles (~71 µm) giving unirradiated cells in the core of those tumors with radii larger than that (*i.e.* r_{tumor}=95 µm), and hence an MCP equal to zero. It can be seen in Figure 3, that in the case of a limited diffusion depth of 30 µm for the activity in the tumors, the limit of the D_{37} for achieving MCP=1 was ~2.2, ~1.3, ~0.6, and ~0.3 Gy for 200, 100, 50, and 25 kBq ^{211}At-MX35 F(ab')2, respectively. The corresponding values for when the activity was homogeneously distributed in the tumor were ~7.5, ~4.8, ~2.8, and ~1.2 Gy.

Tumor growth. Figure 4 shows SEM images of ovarian tumors on the peritoneum in nude mice. The biopsies were taken from the upper left quadrant of the abdominal wall at the time of treatment, *i.e.* four weeks after the intraperitoneal tumor cell inoculation. To simplify the dosimetric and TCP calculations, spherical and cobblestone-surfaced tumors were assumed in all calculations.

Discussion

Calculations of the specific energy delivered to tumor cell nuclei originating from specific binding of the radiolabeled mAbs to the antigenic sites of the tumor cells were first performed for optimal conditions, *i.e.* assuming that all

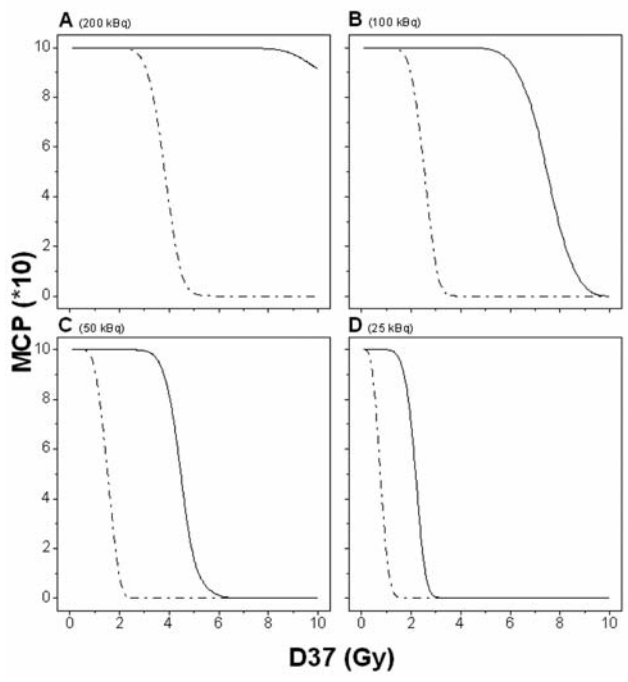

Figure 3. *Metastatic cure probability (MCP) as a function of D_{37} for the various irradiation geometries and for the activity levels of 200 (A), 100 (B), 50 (C), and 25 kBq ^{211}At-MX35 F(ab')2 (D), respectively. Solid line (—): activity homogeneously distributed at all antigenic sites throughout the whole tumor. Dashed line (– –): activity distributed only at antigenic sites located within the assumed maximum diffusion depth (30 μm). The curves for the cases in which the activity is distributed only at antigenic sites on the surface of the tumor or unbound and freely circulating around the tumor were omitted due to the fact that the MCP is zero for all values of D_{37} in those cases. This is explained by the relatively short path length of the α-particles (~71 μm in tissue) resulting in unirradiated cells in the core of tumors with radii larger than that, and hence an MCP equal to zero.*

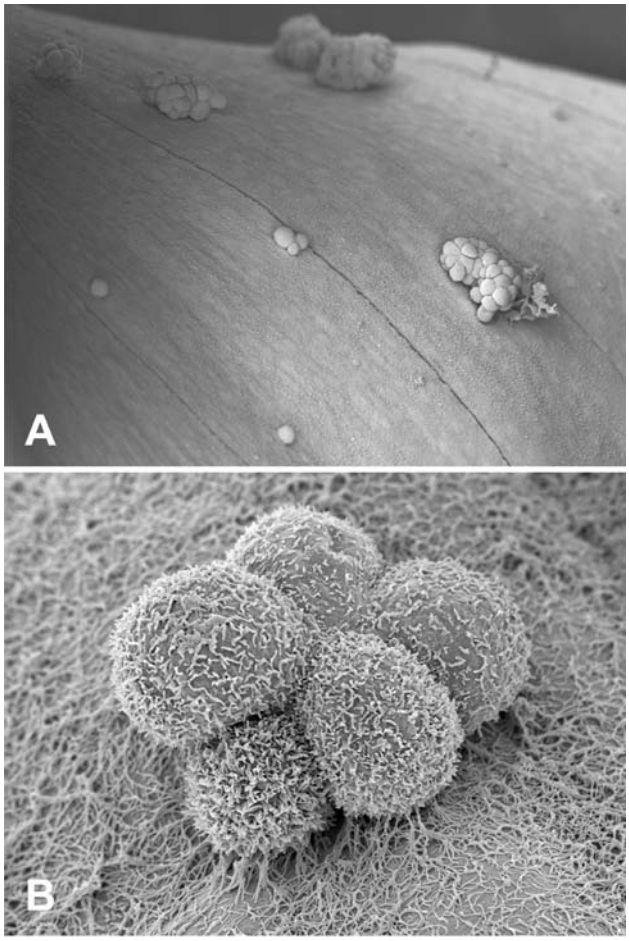

Figure 4. *Scanning electron images showing ovarian cancer cells situated on the peritoneum in nude mice. Panel A shows single cells and a distribution of different tumor sizes four weeks after the intraperitoneal inoculation of the cells. Panel B shows how the cancer cells adhere to the peritoneal surface. In the dosimetric and tumor-cure-probability calculations, the tumors were all considered as spheres with a cobblestone surface.*

tumor cells and antigenic sites in the tumor were available to the mAbs. This situation most probably does not reflect the situation *in vivo*, but was assumed for the purpose of estimating the maximum attainable specific energy delivered to cell nuclei. The specific energy delivered to cell nuclei was also chosen to be calculated for the other extreme, no diffusion at all into the tumor, resulting in a ^{211}At-mAb distribution only on the surface of the tumor. This means that the radiation did not reach the inner part of the tumor when $r_{tumor} > s_{max}$ (*i.e.* the maximum path length of the α-particles, ~71 μm). Among the four irradiation geometries considered in an earlier study, the one assuming a limited diffusion depth of 30 μm agreed best with the therapeutic outcome (24). In that study, a large increase of the MCP (from 0.33 to 0.98) between the 50 and 100 kBq level agreed with an increase in the TFF (from 22% to 50%), between the same activity levels.

In a previous *in vitro* study investigating the radiation sensitivity of NIH:OVCAR-3 cells using ^{211}At, a D_{37} value of 0.56 Gy was reported (30). In another study of the same cell line, an *in vivo* D_{37} value of 1.59 Gy was reached also using ^{211}At (31). As clearly indicated in the results of the present study, the role of the radiation sensitivity of the tumor cells has to be considered during therapy. Molecular and cellular *in vitro* and *in vivo* studies have increased our knowledge regarding the radiosensitivity properties of different tumor cells. It is apparent that no single factor/gene or even cluster of factors/genes determines the degree of radiosensitivity. However, research has demonstrated a variety of factors rendering cells towards either radiosensitive or radioresistant phenotypes. Some of these are already under evaluation as prognostic factors in the

clinic (32, 33). Correlation between EGFR overexpression and radioresistance has been shown both *in vitro* and *in vivo* (34, 35). One of the most studied is the overexpression of the p53 protein. Hamada *et al*. concluded that *p53* mutations are associated with poor response to chemotherapy and radiotherapy (36). Using 16 stable *p53* mutants, Okaichi *et al*. demonstrated that different sites of *p53* mutations result in different degrees of radiosensitivity (6). Increased radioresistance was exhibited among mutants with point mutations in the hotspot regions, most commonly mutated in ovarian cancer cells. The presented theoretical model may aid in the design of successful treatment strategies based on such/identified biological and physical properties. In the case of an assumed limited diffusion depth of 30 μm of the activity in this study, the TCP was high for D_{37} values not exceeding ~4.3, ~2.9, ~1.8, and ~0.8 Gy for 200, 100, 50, and 25 kBq injected ^{211}At-MX35 F(ab')2, respectively. Regarding the MCP in the case of the limited diffusion depth of the activity in the tumors, the limit of D_{37} for achieving MCP=1 was ~2.2, ~1.3, ~0.6, and ~0.3 Gy for 200, 100, 50, and 25 kBq ^{211}At-MX35 F(ab')2, respectively. In humans, these activity levels correspond to ~400, ~200, ~100, and 50 MBq ^{211}At-MX35 F(ab')2, respectively.

Since the research group led by Professor Ragnar Hultborn (Department of Oncology, Sahlgrenska Academy, University of Gothenburg) and Professor Lars Jacobsson (Department of Radiation Physics, Sahlgrenska Academy, University of Gothenburg) just recently published the result of a phase I study on nine women with refractory ovarian cancer using ^{211}At-MX35 F(ab')$_2$ (37), and are now planning for a phase II study, we find it important to investigate different aspects potentially influencing the therapeutic outcome, *e.g*. the radiation sensitivity of the tumor cells investigated in this study.

Conclusion

The radiation sensitivity, expressed as D_{37}, of cells subjected to α-RIT could be decisive for the therapeutic outcome, expressed as TCP or MCP, when treating small tumors of ovarian cancer in mice.

Acknowledgements

Ragnar Hultborn (MD, Ph.D.), Head of the Department of Oncology (Sahlgrenska Academy, University of Gothenburg) is acknowledged for letting us carry out this study through at that department. Stig Palm (Ph.D.) is acknowledged for letting us use published data derived from a computer program developed by him. Kanita Cukur is acknowledged for the preparation of the electron microscopy specimens. This study was supported by grants from the Swedish Cancer Society, the King Gustaf V Jubilee Clinic Research Foundation (Gothenburg, Sweden), and the Assar Gabrielsson Foundation (Gothenburg, Sweden).

References

1 Reedy M, Gallion H, Fowler JM, Kryscio R and Smith SA: Contribution of *BRCA1* and *BRCA2* to familial ovarian cancer: a gynaecological oncology group study. Gynecol Oncol *85*: 255-259, 2002.

2 Aarnio M, Sankila R, Pukkala E, Salovaara R, Aaltonen LA, de la Chapelle A, Peltomäki P, Mecklin JP and Järvinen HJ: Cancer risk in mutation carriers of DNA-mismatch-repair genes. Int J Cancer *81*: 214-218, 1999.

3 Marks JR, Davidoff AM, Kerns BJ, Humphrey PA, Pence JC, Dodge RK, Clarke-Pearson DL, Iglehart JD, Bast RC Jr. and Berchuck A: Overexpression and mutation of *p53* in epithelial ovarian cancer. Cancer Res *51*: 2979-2984, 1991.

4 Fujita M, Enomoto T, Haba T, Nakashima R, Sasaki M, Yoshino K, Wada H, Buzard GS, Matsuzaki N, Wakasa K and Murata Y: Alteration in *p15* and *p16* genes in common epithelial ovarian tumors. Int J Cancer *74*: 148-155, 1997.

5 Harrison LB, Chadha M, Hill RJ, Hu K and Shasha D: Impact of tumor hypoxia and anemia on radiation therapy outcomes. Oncologist *7*: 492-508, 2002.

6 Okaichi K, Ide-Kenematsu M, Izumi N, Morita N, Okumura Y and Ihara M: Variations in sensitivity to ionizing radiation in relation to *p53* mutation point. Anticancer Res *28*: 2687-2690, 2008.

7 McQuarrie S, Mercer J, Syme A, Suresh M and Miller G: Preliminary results of nanopharmaceuticals used in the radioimmunotherapy of ovarian cancer. J Pharm Pharm Sci *7*: 29-34, 2005.

8 Janssen ML, Pels W, Massuger LF, Oyen WJ, Boonstra H, Corstens FH and Boerman OC: Intraperitoneal radioimmunotherapy in an ovarian carcinoma mouse model: Effect of the radionuclide. Int J Gynecol Cancer *13*: 607-613, 2003.

9 Borchardt PE, Quadri SM, Freedman RS and Vriesendorp HM: Intraperitoneal radioimmunotherapy with human monoclonal IGM in nude mice with peritoneal carcinomatosis. Cancer Biother Radiopharm *15*: 53-64, 2000.

10 Grana C, Bartolomei M, Handkiewicz D, Rocca P, Bodei L, Colombo N, Chinol M, Mangioni C, Malavasi F and Paganelli G: Radioimmunotherapy in advanced ovarian cancer: Is there a role for pre-targeting with (90)Y-biotin? Gynecol Oncol *93*: 691-698, 2004.

11 Meredith RF, Alvarez RD, Partridge EE, Khazaeli MB, Lin CY, Macey DJ, Austin JM Jr., Kilgore LC, Grizzle WE, Schlom J and LoBuglio AF: Intraperitoneal radioimmunochemotherapy of ovarian cancer: A phase I study. Cancer Biother Radiopharm *16*: 305-315, 2001.

12 Mahe MA, Fumoleau P, Fabbro M, Guastalla JP, Faurous P, Chauvot P, Chetanoud L, Classe JM, Rouanet P and Chatal JF: A phase II study of intraperitoneal radioimmunotherapy with iodine-131-labeled monoclonal antibody OC-125 in patients with residual ovarian carcinoma. Clin Cancer Res *5(S)*: 3249-3252, 1999.

13 Epenetos AA, Hird V, Lambert H, Mason P and Coulter C: Long-term survival of patients with advanced ovarian cancer treated with intraperitoneal radioimmunotherapy. Int J Gynecol Cancer *10*: 44-46, 2000.

14 Alvarez RD, Partridge EE, Khazaeli MB, Plott G, Austin M, Kilgore L, Russell CD, Liu T, Grizzle WE, Schlom J, Lo Buglio AF and Meredith RF: Intraperitoneal radioimmunotherapy of ovarian cancer with ^{177}Lu-CC49: A phase I/II study. Gyncol Oncol *65*: 94-101, 1997.

15 Alvarez RD, Huh WK, Khazaeli MB, Meredith RF, Partridge EE, Kilgore LC, Grizzle WE, Shen S, Austin JM, Barnes MN, Carey D, Schlom J and LoBuglio AF: A phase I study of combined modality ^{90}yttrium-CC49 intraperitoneal radioimmunotherapy for ovarian cancer. Clin Cancer Res *8*: 2806-2811, 2002.
16 Stewart JS, Hird V, Snook D, B Dhokia, G Sivolapenko, G Hooker, JT Papadimitriou, G Rowlinson, M Sullivan, and HE Lambert: Intraperitoneal yttrium-90-labeled monoclonal antibody in ovarian cancer. J Clin Oncol *8*: 1941-1950, 1990.
17 Seiden M and Benigno BB: The SMART Study Investor Group (Southeastern Gynecological Oncology). A pivotal phase III trial to evaluate the efficacy and safety of adjuvant treatment with R1549 (yttrium-90-labeled HMFG1 murine monoclonal antibody) in epithelial ovarian cancer (EOC). Proc Am Soc Clin Oncol Abstract No. 5008, 2004.
18 Horak E, Hartmann F, Garmestani K, Wu C, Brechbiel M, Gansow OA, Landolfi NF and Waldmann TA: Radioimmunotherapy targeting of HER2/neu oncoprotein on ovarian tumor using lead-212-DOTA-AE1. J Nucl Med *38*: 1944-1950, 1997.
19 Borchardt PE, Yuan RR, Miederer M, McDevitt MR and Scheinberg DA: Targeted actinium-225 *in vivo* generators for therapy of ovarian cancer. Cancer Res *63*: 5084-5090, 2003.
20 Andersson H, Lindegren S, Bäck T, Jacobsson L, Leser G, Horvath G: Radioimmunotherapy of nude mice with intraperitoneally growing ovarian cancer xenograft utilizing ^{211}At-labelled monoclonal antibody MOv18. Anticancer Res *20*: 459-462, 2000.
21 Andersson H, Lindegren S, Bäck T, Jacobsson L, Leser G and Horvath G: The curative and palliative potential of the monoclonal antibody MOv18 labelled with ^{211}At in nude mice with intraperitoneally growing ovarian cancer xenografts: A long term study. Acta Oncol *39*: 741-745, 2000.
22 Andersson H, Palm S, Lindegren S, Bäck T, Jacobsson L, Leser G and Horvath G: Comparison of the therapeutic efficacy of ^{211}At- and ^{131}I-labelled monoclonal antibody MOv18 in nude mice with intraperitoneal growth of human ovarian carcinoma. Anticancer Res *21*: 409-412, 2001.
23 Elgqvist J, Andersson H, Bäck T, Hultborn R, Jensen H, Karlsson B, Lindegren S, Palm S, Warnhammar E and Jacobsson L: Therapeutic efficacy and tumor dose estimations in radioimmunotherapy of intraperitoneally growing OVCAR-3 cells in nude mice with the ^{211}At-labeled monoclonal antibody MX35. J Nucl Med *46*: 1907-1915, 2005.
24 Elgqvist J, Andersson H, Bäck T, Claesson I, Hultborn R, Jensen H, Johansson BR, Lindegren S, Olsson M, Palm S, Warnhammar E and Jacobsson L: Alpha-radioimmunotherapy of intraperitoneally growing OVCAR-3 tumors of variable dimensions: Outcome related to measured tumor size and mean absorbed dose. J Nucl Med *47*: 1342-1350, 2006.
25 Elgqvist J, Andersson H, Bernhardt P, Bäck T, Claesson I, Hultborn R, Jensen H, Johansson BR, Lindegren S, Olsson M, Palm S, Warnhammar E and Jacobsson L: Administered activity and metastatic cure probability during radioimmunotherapy of ovarian cancer in nude mice with ^{211}At-MX35 F(ab')2. Int J Radiat Oncol Biol Phys *66*: 1228-1237, 2006.
26 Palm S, Humm JL, Rundqvist R and Jacobsson L: Microdosimetry of astatine-211 single-cell irradiation: Role of daughter polonium-211 diffusion. Med Phys *31*: 218-225, 2004.
27 ICRU. Stopping powers and ranges for protons and alpha particles. Publication 49. Bethesda, Maryland: International Commission on Radiation Units and Measurements; 1993.
28 Sgouros G: Plasmapheresis in radioimmunotherapy of micrometastases: A mathematical modeling and dosimetrical analysis. J Nucl Med *33*: 2167-2179, 1992.
29 Friedman PL and Ellisman MH: Enhanced visualization of peripheral nerve and sensory receptors in the scanning electron microscope using cryofracture and osmium-thiocarbohydrazide-osmium impregnation. J Neurocytol *10*: 111-131, 1981.
30 Palm S, Andersson H, Bäck T, Claesson I, Delle U, Hultborn R, Jacobsson L, Köpf I and Lindegren S: *In vitro* effects of free ^{211}At, ^{211}At-albumin and ^{211}At-monoclonal antibody compared to external photon irradiation on two human cancer cell lines. Anticancer Res *20*: 1005-1012, 2000.
31 Bäck T, Andersson H, Divgi CR, Hultborn R, Jensen H, Lindegren S, Palm S and Jacobsson L: ^{211}At-radioimmunotherapy of subcutaneous human ovarian cancer xenografts: Evaluation of RBE of an alpha emitter *in vivo*. J Nucl Med *46*: 2061-2067, 2005.
32 Milas L, Fan Z, Andratschke NH and Ang KK: Epidermal growth factor receptor and tumor response to radiation: *in vivo* preclinical studies. Int J Radiat Oncol Biol Phys *58*: 966-971, 2004.
33 Fountzilas G, Kalogera-Fountzila A, Lambaki S, Wirtz RM, Nikolaou A, Karayannopoulou G, Bobos M, Kotoula V, Murray S, Lambropoulos A, Aravantinos G, Markou K, Athanassiou E, Misailidou D, Kalogeras KT and Skarlos D: MMP9 but not EGFR, MET, ERCC1, P16, and P-53 is associated with response to concomitant radiotherapy, cetuximab, and weekly cisplatin in patients with locally advanced head and neck cancer J Oncol *2009*: 305908, 2009.
34 Lammering G, Valerie K, Lin PS, Mikkelsen RB, Contessa JN, Feden JP, Farnsworth J, Dent P and Schmidt-Ullrich RK: Radiosensitization of malignant glioma cells through overexpression of dominant-negative epidermal growth factor receptor. Clin Cancer Res *7*: 682-690, 2001.
35 Huamani J, Willey C, Thotala D, Niermann KJ, Reyzer M, Leavitt L, Jones C, Fleishcher A, Caprioli R, Hallahan DE and Kim DW: Differential efficacy of combined therapy with radiation and AEE788 in high and low EGFR-expressing androgen-independent prostate tumor models. Int J Radiat Oncol Biol Phys *71*: 237-246, 2008.
36 Hamada M, Fujiwara T, Hizuta A, Gochi A, Naomoto Y, Takakura N, Takahashi K, Roth JA, Tanaka N and Orita K: The *p53* gene is a potent determinant of chemosensitivity and radiosensitivity in gastric and colorectal cancers. J Cancer Res Clin Oncol *122*: 360-365, 1996.
37 Andersson H, Cederkrantz E, Bäck T, Divgi C, Elgqvist J, Himmelman J, Horvath G, Jacobsson L, Jensen H, Lindegren S, Palm S and Hultborn R: Intraperitoneal alpha-particle radioimmunotherapy of ovarian cancer patients: pharmacokinetics and dosimetry of ^{211}At-MX35 F(ab')$_2$ – a phase I study. J Nucl Med *50*: 1153-1160, 2009.

Received March 2, 2010
Revised June 3, 2010
Accepted June 8, 2010